

Gravitational Microlensing: A Tool for Detecting and Characterizing Free-Floating Planets

Cheongho Han, Sun-Ju Chung, Doeon Kim

*Department of Physics, Institute for Basic Science Research, Chungbuk National University, Chongju 361-763, Korea;
cheongho,sjchung,dekim@astroph.chungbuk.ac.kr*

Byeong-Gon Park

*Bohyeonsan Optical Astronomy Observatory, Korea Astronomy Observatory, Youngchon 770-820, Korea;
bgpark@boao.re.kr*

Yoon-Hyun Ryu

*Department of Astronomy & Atmospheric Science, Kyungpook National University, Daegu 702-701, Korea;
yhyu@rose0.knu.ac.kr*

Sangjun Kang

School of Liberal Arts, Semyung University, Jechon 390-711, Korea; sjkang@semyung.ac.kr

Dong Wook Lee

*Astrophysical Research Center for the Structure and Evolution of the Cosmos (ARCSEC"), Sejong University, Seoul
143-747, Korea; dwlee@arcsec.sejong.ac.kr*

ABSTRACT

Various methods have been proposed to search for extrasolar planets. Compared to the other methods, microlensing has unique applicabilities to the detections of Earth-mass and free-floating planets. However, the microlensing method is seriously flawed by the fact that the masses of the detected planets cannot be uniquely determined. Recently, Gould, Gaudi, & Han introduced an observational setup that enables one to resolve the mass degeneracy of the Earth-mass planets. The setup requires a modest adjustment to the orbit of an already proposed microlensing planet-finder satellite combined with ground-based observations. In this paper, we show that a similar observational setup can also be used for the mass determinations of free-floating planets with masses ranging from $\sim 0.1 M_J$ to several Jupiter masses. If the proposed observational setup is realized, the future lensing surveys will play important roles in the studies of Earth-mass and free-floating planets, which are the populations of planets that have not been previously probed.

Subject headings: gravitational lensing – planets and satellites: general

1. Introduction

High-precision radial velocity measurements of nearby stars resulted in the detections of more than 100 planetary systems (<http://cfa-www.harvard.edu/planets>). Besides the radial velocity method, planets can also be detected and characterized by using various other methods. These methods include the pulsar timing analysis, direct imaging, accurate measurement of astrometric displacement, planetary transit, and microlensing (see the review of Perryman 2000).

However, all these methods except the microlensing method can be used to detect only planets which are gravitationally bound to their parent stars. Theories about the planet formation indicate that planets often do not stay in the same orbit where they were formed. Dynamical interactions with either a massive planetesimal disk (Murray et al. 1998; Trilling, Levine, & Benz 2002) or the protoplanetary nebular gas (Ward 1997) can result in inward migration of planets. On the other hand, gravitational interactions with other planet members (Levison, Lissauer, & Duncan 1998) or neighboring

stars (Sigurdsson 1992) can result in the disruption of the planetary system and thus ejection of planets. The latter process could lead to a population of free-floating planets.

Microlensing can be occurred by a low-mass object and thus free-floating planets can be, in principle, searched for by detecting short-duration lensing-induced light variations of background stars caused by the planets. However, this method has not been used due to technical difficulties. These difficulties arise because of the rarity of lensing events combined with the short durations of planetary events. At any given time, only a few out of 10^6 Galactic bulge stars undergo microlensing with their fluxes magnified enough for detection and a small fraction of those microlensed stars are expected to be lensed by planetary masses. In addition, events produced by planetary lenses last only a short duration of ~ 1 day even for an event caused by a giant planet (with a mass $M \sim 10^{-3} M_\odot$) and the duration decreases in proportional to the square root of the lens mass. Therefore, implementing the microlensing method to search for free-floating planets requires a massive survey for a large number of stars with a very high monitoring frequency. Several groups have been previously carried out and are currently performing lensing surveys (Alcock et al. 1993; Aubourg et al. 1993; Udalski et al. 1993; Alard & Guibert 1997; Bond et al. 2002), but the typical monitoring frequency of these experiments is at most several times per day, which is far too low to detect events caused free-floating planets. To increase the monitoring frequency, the experiments are employing early warning systems (Alcock et al. 1996; Afonso et al. 2001; Bond et al. 2001; Udalski et al. 1994) to issue alerts of ongoing events detected in the early stage of lensing magnification and follow-up observation programs (Alcock et al. 1997; Rhie et al. 1999; Albrow et al. 1998; Yoo et al. 2003) to intensively monitor the alerted events hoping to detect short-duration planetary signals on the top of the lensing light curve produced by the parent star. However, planets detectable from this type of strategy are also bound planets like the ones detectable from other planet search methods.

However, the situation will greatly change with the advent of future lensing surveys with very high monitoring frequencies. Actually, several such experiments in space and on the ground were proposed. The space-based GEST mission, proposed to NASA by Bennett & Rhie (2002), is designed to continuously monitor $\sim 10^8$ Galactic bulge main-sequence stars with a frequency of several times per hour by using a 1–2 m aperture space telescope. Studies about the scientific outcome from a ground-based high-frequency lensing experiment using four 2 m-class telescopes located at good seeing sites around the world and equipped with large format CCD cameras are in progress (Gould, Gaudi, & Han 2003). From detailed simulations of Galactic bulge events detectable from the

space observation by using the GEST, Bennett & Rhie (2002) estimated that the total number of detections of events caused by free-floating planets during the life time of the GEST mission (~ 3.7 yrs) would be $\sim (\mathcal{O})10$ for Earth-mass planets and $\sim (\mathcal{O})10^2$ for giant planets under the assumption that one planet was ejected for each star.

However, the microlensing method is seriously flawed by the fact that the detected planet’s mass cannot be uniquely determined. This defect arises because among the three lensing observables related to the physical parameters of the lens, the Einstein time scale t_E , the angular Einstein ring radius θ_E , and the projected Einstein radius onto the plane of the observer \tilde{r}_E , only t_E is routinely measured from the lensing light curve. These three observables are related to the mass of the lens (M), relative source-lens parallax ($\pi_{rel} = \text{AU}/[D_l^{-1} - D_s^{-1}]$, where D_l and D_s are the distances to the lens and source, respectively), and proper motion (μ_{rel}) by (Gould 2000)

$$t_E = \frac{\theta_E}{\mu_{rel}}, \quad \theta_E = \sqrt{\frac{4GM\pi_{rel}}{c^2 \text{AU}}}, \quad \tilde{r}_E = \sqrt{\frac{4GM \text{AU}}{c^2\pi_{rel}}}. \quad (1)$$

Due to the fact that t_E results from the combination of M , π_{rel} , and μ_{rel} , short durations of events do not guarantee the events are caused by planets because they can be produced by low-mass stars or brown dwarfs with exceptionally high proper motions or very small Einstein ring radii. As a result, even if a large number of short-duration events were detected by future lensing surveys, they could not be definitely identified as planetary events. To isolate events caused by free-floating planets and determine their masses, it is required to measure the other observables of θ_E and \tilde{r}_E (see § 2 for the detailed description about the methods to measure these quantities). Once θ_E and \tilde{r}_E are measured, the lens mass is uniquely determined by

$$M = \frac{c^2}{4G} \tilde{r}_E \theta_E. \quad (2)$$

Recently, Gould, Gaudi, & Han (2003) pointed out that the masses of *bound* Earth-mass planets could be measured by combining a GEST-type satellite with ground-based observations. They showed that the proper motions of these events can be measured by analyzing the planet-induced perturbations in lensing light curves observed from space. They also showed that if the satellite is placed in an L2 orbit, the Earth-satellite baseline is sufficient enough to measure lens parallaxes. In this paper, we show that a similar observational setup proposed by Gould, Gaudi, & Han (2003) can also be used for the mass determinations of free-floating planets, which are the population of planets that have not been previously probed.

The paper is organized as follows. In § 2, we describe the methods of \tilde{r}_E and θ_E measurements and explain the

reasons for the difficulties in measuring these quantities for events caused by stellar mass lenses. In § 3, we illustrate the relative easiness of \tilde{r}_E and θ_E measurements for events caused by low-mass lenses such as free-floating planets. In § 4, we estimate the mass range over which the proposed mass determination method is sensitive by estimating the uncertainties of the recovered lens masses under the observational setup proposed by Gould, Gaudi, & Han (2003). In § 5, we briefly discuss several problems of the proposed observational setup. We conclude in § 6.

2. Mass Determinations of Gravitational Lenses

A microlensing event occurs when a compact massive object (lens) approaches very close to the observer’s line of sight toward a background star (source). Due to the lensing-induced magnification and the varying lens-source separation caused by the relative proper motion, the source star flux changes with time. For an event involved with a point source, the magnification of the source star flux varies with time by

$$A = \frac{u^2 + 2}{u\sqrt{u^2 + 4}}; \quad \mathbf{u} = \left(\frac{t - t_0}{t_E} \right) \hat{\mathbf{x}} + u_0 \hat{\mathbf{y}}, \quad (3)$$

where \mathbf{u} represents the lens-source separation vector normalized by θ_E , u_0 is the closest lens-source separation in units of θ_E (impact parameter), t_0 is the time at that moment (time of maximum magnification), and $\hat{\mathbf{x}}$ and $\hat{\mathbf{y}}$ are the unit vectors parallel with and normal to the direction of the lens-source motion, respectively. Among the three lensing parameters of a point-source event (t_0 , u_0 and t_E), the first two tell nothing about the lens and the third is related to M , π_{rel} , and μ_{rel} in a complicated way presented in equation (1). To fully break the lens parameter degeneracy, two additional pieces of information of θ_E and \tilde{r}_E are needed.

The angular Einstein ring radius can be measured by scaling θ_E against some known “standard angular rulers” on the source plane (the plane perpendicular to the line of sight toward the source at the position of the source). The most ubiquitous standard ruler is the source star itself. If the lens passes close enough to the source, the source star can no longer be approximated as a point source. In this case, different parts on the source star surface are magnified by different amounts due to the difference in separation from the lens, and the resulting light curve deviates from that of a point source event; finite source effect (Witt & Mao 1994). By measuring the deviation caused by the finite source effect, one can measure the relative source size normalized by the angular Einstein ring radius, $\rho_* = \theta_*/\theta_E$ (normalized source radius), where θ_* is the angular radius of the source star. Since θ_* can be estimated from the position of the source star on a color-magnitude diagram (CMD) relative to the center of red clump giants, whose dereddened and calibrated position on the CMD is well known (An et al.

2002; van Belle 1999), the angular Einstein ring radius is determined by $\theta_E = \theta_*/\rho_*$ (Gould 1994a; Nemiroff & Wickramasinghe 1994).

The projected Einstein ring radius can be measured by scaling \tilde{r}_E against some known “standard physical rulers” on the plane of the observer (the plane perpendicular to the line of sight toward the source at the position of the observer). Such a standard ruler is provided by observing an event at two different locations. If an event is seen by two observers located at different locations, the source star position with respect to the lens is different. The amount of the normalized difference between the source positions is

$$\Delta \mathbf{u} = \frac{\tilde{\mathbf{d}}}{\tilde{r}_E}, \quad (4)$$

where $\tilde{\mathbf{d}}$ is the separation vector between the two observers projected onto the observer plane. Then, if $\tilde{\mathbf{d}}$ is large enough, the light curves of the event seen from the two observers will exhibit noticeable differences; parallax effect (Refsdal 1966; Gould 1992). By measuring the difference in impact parameters, Δu_0 , and the difference in times of maximum magnification, Δt_0 , between the light curves as seen from the two observers, one can measure $\Delta \mathbf{u} = (\Delta t_0/t_E, \Delta u_0)$, and so \tilde{r}_E (with the known separation vector $\tilde{\mathbf{d}}$).

However, determining the lens masses by using the mentioned standard rulers for events caused by stellar mass lenses was not easy. This is because the Einstein ring radii of these events are much larger than the sizes of the rulers. For Galactic bulge events, the sizes of θ_E and \tilde{r}_E are

$$\theta_E = 1.26 \text{ mas} \left(\frac{D_s}{D_l} - 1 \right)^{1/2} \left(\frac{D_s}{8 \text{ kpc}} \right)^{-1/2} \left(\frac{M}{M_\odot} \right)^{1/2}, \quad (5)$$

and

$$\tilde{r}_E = 8.2 \text{ AU} \left(\frac{D_s}{D_l} - 1 \right)^{-1/2} \left(\frac{D_s}{8 \text{ kpc}} \right)^{1/2} \left(\frac{M}{M_\odot} \right)^{1/2}. \quad (6)$$

Noticeable light curve deviations caused by the finite source effect are produced only when the lens-source separation is equivalent to or less than the source radius (see Figure 2). However, the normalized source radius of a typical bulge event caused by a stellar mass lens with $M \sim 0.3 M_\odot$ located at $D_l = 6 \text{ kpc}$ is merely $\rho_* \sim 0.0018$ for a main-sequence star (with a physical radius of $R_* \sim 1 R_\odot$ and an angular size of $\theta_* \sim 0.6 \mu\text{arcsec}$ at $D_s \sim 8 \text{ kpc}$) and $\rho_* \sim 0.02$ even for a clump giant star (with $R_* \sim 13 R_\odot$ and $\theta_* \sim 7.6 \mu\text{arcsec}$). This implies that close lens-source approach enough to produce noticeable light curve deviations caused by the finite source effect occurs very rarely and thus one can measure θ_E only for a very small fraction of events. In addition, the typical projected Einstein ring radius for these events is

$\tilde{r}_E \sim 7.6$ AU, and thus measurement of \tilde{r}_E is impossible with an Earth-scale baseline.¹ One may think an appropriate baseline can be provided by a satellite with a heliocentric orbit. However, the problem of this solution is that transmission of a huge amount of data from the satellite is difficult with the current technology. In addition, even if the technical problem is resolved and events are observed from the Earth and the satellite, still \tilde{r}_E cannot be uniquely determined because of the inherent degeneracy in Δu . This degeneracy arises because for a given pair of light curves observed from the two different locations there can be two possible values of Δu depending on whether the source star trajectories as seen from the Earth and the satellite are on the same or opposite sides with respect to the lens, causing a two-fold degeneracy in the determined value of \tilde{r}_E (Gould 1994b). To lift this degeneracy, one needs a second satellite. As a result, θ_E and \tilde{r}_E have been measured for only a handful number of events each out of the more than 1000 events detected so far [Alcock et al. (1997, 2000); Albrow et al. (1999, 2000, 2001); Afonso et al. (2000); Yoo et al. (2003) for θ_E measurements and Alcock et al. (1995); Mao (1999); Soszyński et al. (2001); Bond et al. (2001); Mao et al. (2002); Bennett (2002) for \tilde{r}_E measurements], and for only a single event both θ_E and \tilde{r}_E have been measured (An et al. 2002).²

3. Events Caused by Free-Floating Planets

Unlike events caused by stellar mass lenses, it is possible to measure both \tilde{r}_E and θ_E for a substantial fraction of events caused by free-floating planets. This is because the Einstein ring radii of these events are much smaller than those of the events produced by stellar mass lenses. Then, the sizes of the angular and physical standard rulers on the source and observer planes compared to θ_E and \tilde{r}_E , respectively, are no longer negligible, and thus the events are more susceptible to both the finite-source and parallax effects.

3.1. Parallax Effect

If an event caused by a free-floating planet is observed simultaneously from the Earth and a satellite located at a distance of $d \sim 0.01$ AU, corresponding to the distance to a satellite located in the L2 orbit, the expected displacement between the locations of the source caused by the parallax effect for a typical bulge event (with $D_s \sim 8$

kpc and $D_s \sim 6$ kpc) would be

$$\Delta u = \frac{d \cos \psi}{\tilde{r}_E} \sim 0.02 \cos \psi \left(\frac{M}{M_J} \right)^{-1/2}, \quad (7)$$

where $\cos \psi$ is the projection factor. Although this shift is significantly larger than the shift expected from the event caused by a stellar mass lens, it is still small compared to θ_E . Then, one may question whether the light curves observed from the Earth and the satellite can exhibit noticeable differences with such a small displacement.

For high magnification events, however, the light curve difference induced by the parallax effect can be large even with a small amount of Δu . The reason can be analytically explained as follows. Differentiating the expression of the magnification in equation (3) with respect to u yields

$$\frac{dA}{du} = -\frac{8}{u^2(u^2 + 4)^{3/2}}. \quad (8)$$

Then the fractional difference between the light curves seen from the Earth and the satellite is computed by

$$\epsilon_\pi = \frac{A_{sat} - A_\oplus}{A_\oplus} \sim \frac{\Delta u}{A_\oplus} \left| \frac{dA_\oplus}{du} \right| = \frac{8\Delta u}{u(u^2 + 2)(u^2 + 4)}, \quad (9)$$

where A_\oplus and A_{sat} represent the magnifications measured from the Earth and the satellite, respectively. For a high magnification event ($u \rightarrow 0$), equation (9) is simplified into the form

$$\epsilon_\pi \sim \frac{\Delta u}{u}. \quad (10)$$

From equation (10), one finds that even with a small amount of Δu , the deviation can be large for high magnification events. For example, the fractional difference between the light curves caused by the source star's positional displacement of $\Delta u = 0.02$ is $\epsilon_\pi \gtrsim 5\%$ for events with $u_0 \lesssim 0.4$, implying that the difference can be measured for a significant fraction of events caused by free-floating planets.

The feasibility of parallax measurements for high magnification events is illustrated in Figure 1, where we present light curves of an example planetary event observed from the Earth (solid curve) and a satellite (dotted curves). The event as seen from the Earth has an impact parameter of $u_0 = 0.2$ and the source position as seen from the satellite is slightly displaced by $\Delta u_0 = 0.02/\sqrt{2}$ and $\Delta t_0/t_E = 0.02/\sqrt{2}$ (and thus $\Delta u = \sqrt{(\Delta t_0/t_E)^2 + \Delta u_0^2} = 0.02$). The inset on the left corner of the upper panel shows the geometry of the lens system, where the dashed circle represents the Einstein ring and the solid and dotted straight lines represent the source star trajectories as seen from the Earth and the satellite, respectively, with respect to the lens (marked by a small filled dot at the center of the Einstein ring).

¹For an event with a very long time scale ($t_E \gtrsim 100$ days), it is possible to measure \tilde{r}_E because the location of the observer changes considerably during the event because of the orbital motion of the Earth around the Sun.

²We note that most of the events for which θ_E are measured are caustic-crossing binary lens events, which comprise only a small fraction of the total number of events. We also note that all of the events with known parallaxes are very long time-scale events, which comprise also a small fraction of the total number of events.

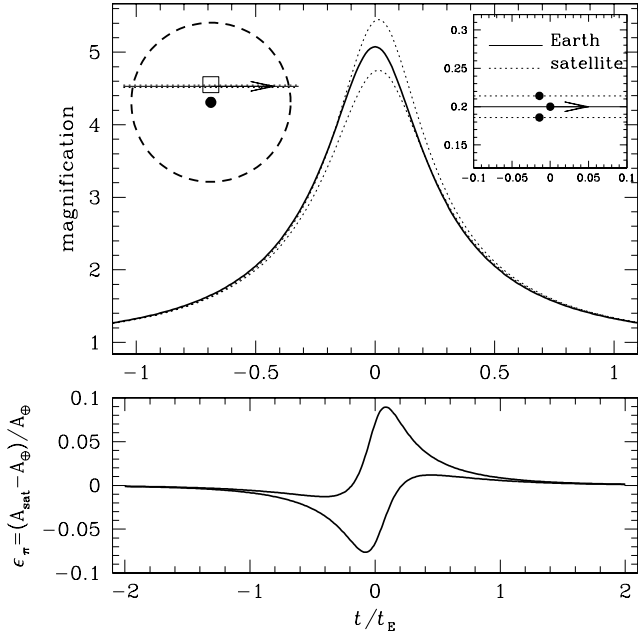


Fig. 1.— Upper panel: Light curves of an example planetary event observed from the Earth (solid curve) and a satellite (dotted curves). The inset on the left corner shows the geometry of the lens system, where the dashed circle represents the Einstein ring and the solid and dotted straight lines represent the source star trajectories as seen from the Earth and the satellite, respectively, with respect to the lens (marked by a small filled dot at the center of the Einstein ring). The inset on the right corner shows the blowup of the region enclosed by a square on the left-side inset. The three dots represent the source locations at the moment when the magnification of the event seen from the Earth is maximum. Lower panel: Fractional difference between the light curves.

The inset on the right corner shows the blowup of the region enclosed by a square in the left-side inset. The three dots represent the source locations at the moment when the magnification of the event seen from the Earth is maximum, i.e. $t = t_0$. The lower panel shows the fractional deviation ϵ_π . One finds that even with a very small displacement of the source trajectory, the deviation is as large as $\epsilon_\pi \sim 10\%$ as predicted by equation (10).

We note that the parallax of the event caused by a free-floating planet does not suffer from the degeneracy mentioned in § 2. This is because the source trajectory seen from the Earth and the satellite are nearly always located on the same side with respect to the lens due to the small value of Δu expected for typical planetary events.

3.2. Finite Source Size Effect

High-magnification planetary events are susceptible not only to the parallax effect but also to the finite source

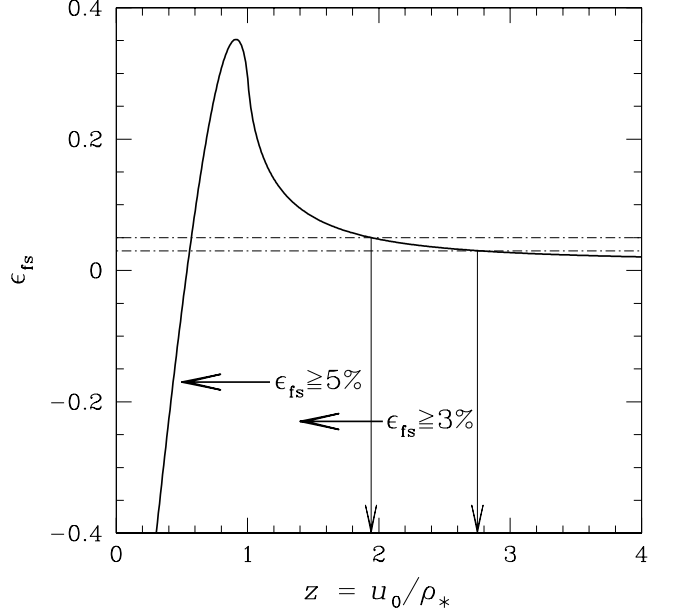


Fig. 2.— Fractional deviation of the lensing magnification caused by the finite source effect as a function of $z = u_0/\rho_*$, where u_0 and ρ_* represent the normalized impact parameter of the lens-source encounter and the normalized source radius. Then, $z < 1$ ($u_0 < \rho_*$) implies that the lens transverse the source star surface.

effect. The light curve affected by the finite source effect is given by the intensity-weighted magnification averaged over the source flux. Under the assumption of a uniform source brightness, the magnification of an event affected by the finite source effect is expressed by

$$A_{fs} = \frac{1}{\pi \rho_*^2} \int_0^{2\pi} d\theta \int_0^{\rho_*} d\rho \rho A \left[\sqrt{(u_c + \rho \cos \theta)^2 + (\rho \sin \theta)^2} \right], \quad (11)$$

where u_c represents the normalized separation between the lens and the center of the source star, and ρ and θ represent the position vector and the position angle of a point on the source star surface with respect to the source star's center, respectively. In the case of a high magnification event, for which the finite source effect is important, the magnification is approximated by

$$A \sim \frac{1}{u}. \quad (12)$$

Using equations (11) and (12), one finds the expression for the ratio between the magnifications with and without the finite source effect, i.e.

$$\frac{A_{fs}}{A} \sim B(z) = \frac{z^2}{\pi} \int_0^{2\pi} d\theta \int_0^{1/z} d\zeta \frac{\zeta}{\sqrt{\zeta^2 + 2\zeta \cos \theta + 1}}, \quad (13)$$

where $z = u/\rho_*$ (Gould 1994a). Then, the fractional deviation caused by the finite source effect is expressed

in terms of the function $B(z)$ as

$$\epsilon_{fs} = \frac{A_{fs} - A}{A} \sim B(z) - 1. \quad (14)$$

In Figure 2, we present the fractional deviation caused by the finite source effect as a function of z . From the curve, one finds that if the lens approaches the source star closer than ~ 1.9 and ~ 2.7 times of the source star radius, the deviations become $\epsilon_{fs} \gtrsim 5\%$ and $\gtrsim 3\%$, respectively. The normalized angular radius of a Galactic bulge main-sequence source star (with a physical size of $R_\star \sim 1 R_\odot$ and an angular size of $0.6 \mu\text{arcsec}$ at $D_s \sim 8 \text{ kpc}$), which is the main monitoring target of the GEST mission, is $\rho_\star \sim 0.032(M/M_J)^{-1/2}$. Then, with a detection condition of $\epsilon_{fs} \geq 3\%$, the deviation can be detected for events with $u_0 \lesssim 2.7 \times 0.032(M/M_J)^{-1/2} \sim 0.086(M/M_J)^{-1/2}$. Note that while one needs both light curves obtained from the Earth and the satellite for \tilde{r}_E measurement, θ_E can be measured from a single light curve obtained from space observation with exquisite photometry.

4. Sensitivity: Quantitative Analysis

As the mass of the lens decreases, the resulting event becomes more susceptible to the parallax effect for a given baseline and to the finite source effect for a given source radius. However, if the lens mass is too small, the detection efficiency of the deviation will sharply drop and the uncertainty of the determined lens mass will become large due to not-enough coverage of the deviation. In this section, we estimate the lens mass range over which the proposed method is sensitive. For this, we estimate the uncertainties of \tilde{r}_E and θ_E expected under the observational setup proposed by Gould, Gaudi, & Han (2003).

To determine the uncertainties of \tilde{r}_E and θ_E , we first estimate the uncertainties of the lensing parameters. We estimate these uncertainties by computing the curvature matrix of χ^2 surface, c_{ij} . For the case of a microlensing light curve, the curvature matrix is defined by

$$c_{ij} = \sum_k^{N_{obs}} \frac{\partial F_{obs,k}}{\partial p_i} \frac{\partial F_{obs,k}}{\partial p_j} \frac{1}{\sigma_k^2}, \quad (15)$$

where N_{obs} is the number of observations, $F_{obs,k}(t) = A(t)F_s + F_b$ is the observed flux for each measurement, $p_i = (F_s, F_b, u_0, t_0, t_E, \rho_\star)$ are the lensing parameters, F_s and F_b are the fluxes of the lensed source star and blended light, and σ_k is the photometric uncertainty of each measurement. We note that in addition to the lensing parameters of a point-source event, two additional parameters of F_b and ρ_\star are included to account for the blending and finite source effects. Then, the uncertainties of the individual lensing parameters correspond to the diagonal components of the inverse curvature matrix

(covariance matrix $b = c^{-1}$, where $\sum_k b_{ik}c_{kj} = \delta_{ij}$), i.e.

$$\sigma_{p_i} = \sqrt{b_{ii}}. \quad (16)$$

The error analysis is done for events with a source and a lens located at 8 kpc and 6 kpc, respectively, and varying the lens mass and u_0 . The assumed relative proper motion is $\mu_{rel} = 7.0 \text{ mas/yr}$ (corresponding to the relative lens-source transverse speed of $v_{rel} = 200 \text{ km s}^{-1}$). Then, the corresponding event time scale is $t_E = 0.96 \text{ days } (M/M_J)^{1/2}$. The proposed GEST mission will take images of Galactic bulge main-sequence stars with 2 min exposure and coadd 5 images to yield 10 min exposure (Bennett & Rhie 2002). Following the specification of the GEST mission, we assume that each combined image is obtained every 20 min (corresponding to a monitoring frequency of 72/day) considering the data readout time. We also assume a similar monitoring frequency for the ground observation. We assume each event is observed during $-2t_E \leq t_{obs} < 2t_E$. For the photometric uncertainties, we assume 1% and 2% photometry for the space and ground observations, respectively. We also assume that blended light comprises 0% (no blending) and 30% of the observed flux for the space and ground observations, respectively. The source star is assumed to have a solar radius.

Once σ_{p_i} expected from the space and ground observations are determined, the uncertainty of the source trajectory displacement (Δu) is computed according to error propagation analysis by

$$\sigma_{\Delta u} \sim \frac{[\sigma_{\Delta t_0/t_E}^2 (\Delta t_0/t_E)^2 + \sigma_{\Delta u_0}^2 \Delta u_0^2]^{1/2}}{\Delta u}, \quad (17)$$

where $\sigma_{\Delta t_0/t_E}$ and $\sigma_{\Delta u_0}$ are the uncertainties of the differences between the t_0/t_E 's and u_0 's measured from the two light curves obtained from the space and ground observations. To prevent confusion in notations, we note that “ σ ” is used to denote the measurement uncertainty, while “ Δ ” is used to denote the difference in lensing parameters determined from the light curves obtained from the space and ground observations. The uncertainties $\sigma_{\Delta t_0/t_E}$ and $\sigma_{\Delta u_0}$ are computed from σ_{p_i} 's estimated from curvature matrix analysis by

$$\sigma_{\Delta t_0/t_E}^2 \sim \left[\left(\frac{\sigma_{t_E}}{t_E} \right)_{sat}^2 + \left(\frac{\sigma_{t_E}}{t_E} \right)_{\oplus}^2 \right] \left(\frac{\Delta t_0}{t_E} \right)^2, \quad (18)$$

$$\sigma_{\Delta u_0}^2 \sim (\sigma_{u_0})_{sat}^2 + (\sigma_{u_0})_{\oplus}^2,$$

where the subscripts “*sat*” and “ \oplus ” are used to denote uncertainties from space and ground measurements, respectively. The first relation in equation (18) is obtained under the assumption that the uncertainty of $\sigma_{\Delta t/t_E}$ is dominated by σ_{t_E} , i.e. $\sigma_{t_E} \gg \sigma_{t_0}$. To account for the projection effect of the Earth-satellite separation, we assume $\tilde{d} = d/2 = 0.005 \text{ AU}$ and the displacement vector of

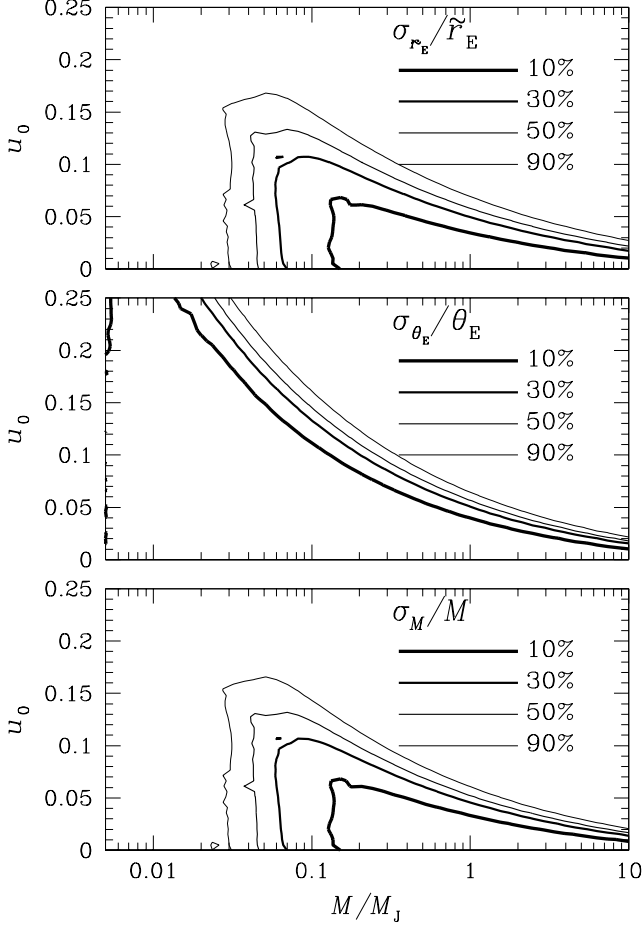


Fig. 3.— Contours maps of the fractional uncertainties of \tilde{r}_E (upper panel), θ_E (middle panel), and the lens mass (lower panel) in the parameters space of (u_0, M) .

the tested event is assumed to have equal x and y components, i.e. $\Delta t_0/t_E = \Delta u_0 = \Delta u/\sqrt{2}$. Since the normalized source star radius can be determined from the light curve observed from space alone, its uncertainty is given simply by

$$\sigma_{\rho_*} = (\sigma_{\rho_*})_{sat}. \quad (19)$$

Once $\sigma_{\Delta u}$ and σ_{ρ_*} are determined, the fractional uncertainties of \tilde{r}_E , θ_E , and the resulting lens mass are obtained by

$$\begin{aligned} \frac{\sigma_{\tilde{r}_E}}{\tilde{r}_E} &\sim \frac{\sigma_{\Delta u}}{\Delta u}, \\ \frac{\sigma_{\theta_E}}{\theta_E} &\sim \frac{\sigma_{\rho_*}}{\rho_*}, \\ \frac{\sigma_M}{M} &\sim \left[\left(\frac{\sigma_{\tilde{r}_E}}{\tilde{r}_E} \right)^2 + \left(\frac{\sigma_{\theta_E}}{\theta_E} \right)^2 \right]^{1/2}. \end{aligned} \quad (20)$$

In Figure 3, we present the estimated uncertainties for \tilde{r}_E (upper panel), θ_E (middle panel), and the lens mass (lower panel) as contours maps in the parameters

space of (u_0, M) . In each map, contours are drawn at the levels of the fractional uncertainties of 10%, 30%, 50%, and 90%. From the figure, one finds that the proposed method is most sensitive to planets with masses ranging from $M \sim 0.1 M_J$ to several Jupiter masses. One also finds that while σ_{θ_E} for a given value of u_0 decreases with the decrease of the lens mass until the lens mass is $M \sim 0.01 M_J$ (equivalent to the mass of an Earth-mass planet), at which the coverage of the deviation becomes less sufficient, the rapid increase of $\sigma_{\tilde{r}_E}$ occurs at a substantially larger mass of $M \sim 0.1 M_J$. As a result, the uncertainty in the determined lens mass for planets with $M \lesssim 1.0 M_J$ is mostly dominated by $\sigma_{\tilde{r}_E}$ rather than σ_{θ_E} . The uncertainty $\sigma_{\tilde{r}_E}$ estimated from the numerical analysis is larger than the expectation based on analytic analysis in § 3.1. To track down the difference, we did the same curvature matrix analysis to determine $\sigma_{\tilde{r}_E}/\tilde{r}_E$ but not taking account the finite source effect (and thus ρ_* is excluded from the list of fitting parameters). From this, we find significant decrease of $\sigma_{\tilde{r}_E}/\tilde{r}_E$ with the decrease of the number of fitting parameters. We find a similar trend when the blending effect is not taken into consideration. We, therefore, conclude that the larger uncertainty $\sigma_{\tilde{r}_E}/\tilde{r}_E$ obtained from the numerical analysis compared to the simple analytic analysis is due to the increase of the number of fitting parameters that are additionally included to account for the blending and the finite source effects (i.e. F_b and ρ_*).

5. Discussion

Considering the high sampling rate with a large format CCD camera, the total data rate of the space microlensing survey will be large, and thus the data transmission from the satellite even at the L2 position will be still a major concern. One way to alleviate the problem is putting a satellite in a highly elliptical orbit with a period of ~ 1 month as proposed by Gould, Gaudi, & Han (2003). Then, the satellite would spend majority of its time near $2a \sim 0.005$ AU and it could focus on data transmission during the brief perigee each month.

Another concern for the proposed satellite observation is the location of the Galactic bulge field in ecliptic coordinates, which are $\lambda = 266^\circ.84$ and $\beta = -5^\circ.54$. Then, while the physical distance to the L2 point is $d \sim 0.01$ AU, the projected separation is very small ($\bar{d} \sim 0.001$ AU) around the time of summer solstice, when the terrestrial observation is optimal. Therefore, during this time of the year, it would be impossible to measure the lens parallax by using the proposed method. However, the bulge season lasts more than ~ 6 months and the survey can be initiated before spring equinox and can be extended after autumnal equinox, at which the projected Earth-satellite separation is maximized. Therefore, lens parallaxes can be measured for a large fraction of the observation time.

We note that the actual uncertainty of the mass measurements will be larger than our estimation because we did not include the uncertainty of the angular source size. There is no empirical calibration of stellar size for main-sequence stars because it is beyond the limit of current interferometric measurements and the available stellar size calibration for these stars are entirely based on theoretical stellar atmosphere calculations. In addition, the uncertainty of the distance to the source star will also contribute to the uncertainty of the mass determinations for free-floating planets.

6. Conclusion

We propose an observational setup that enables one to determine the masses of free-floating planets via gravitational microlensing. The setup is similar to the one of Gould, Gaudi, & Han (2003) proposed to resolve the mass degeneracy of the Earth-mass planets and requires a modest adjustment to the orbit of an already proposed microlensing planet-finder satellite combined with ground-based observations. The proposed method is most sensitive to planets with masses ranging from $\sim 0.1 M_J$ to several Jupiter masses. If realized, the proposed high-frequency lensing surveys will be able to play important roles in characterizing Galactic free-floating planets that have not been probed before.

We would like to thank B. S. Gaudi and A. Gould for making helpful comments. This work was supported by the Astrophysical Research Center for the Structure and Evolution of the Cosmos (ARCSEC²) of Korea Science & Engineering Foundation (KOSEF) through Science Research Program (SRC) program.

REFERENCES

- Afonso, C., et al. 2001, *ApJ*, 532, 340
— 2001, *A&A*, 378, 1014
Alard, C., & Guibert, J. 1997, *A&A*, 326, 1
Albrow, M., et al. 1998, *ApJ*, 509, 687
— 1999, *ApJ*, 512, 672
— 2000, *ApJ*, 534, 894
— 2001, *ApJ*, 549, 759
Alcock, C., et al. 1993, *Nature*, 365, 621
— 1995, *ApJ*, 454, L125
— 1996, *ApJ*, 463, L67
— 1997, *ApJ*, 491, 436
— 2000, *ApJ*, 541, 270
An, J.H., et al. 2002, *ApJ*, 572, 521
Aubourg, E. 1993, *Nature*, 365, 623
Bennett, D.P., & Rhie, S.H. 2002, *ApJ*, 574, 985
Bennett, D.P., et al. 2002, *ApJ*, 579, 639
Bond, I., et al. 2001, *MNRAS*, 327, 868
— 2002, *MNRAS*, 331, L19
Gould, A. 1992, *ApJ*, 392, 442
— 1994a, *ApJ*, 421, L71
— 1994b, *ApJ*, 421, L75
— 2000, *ApJ*, 542, 785
Gould, A., Gaudi, B.S., & Han, C. 2003, *ApJ*, 591, L53
Levison, H.F., Lissauer, J.J., & Duncan, M.J. 1998, *AJ*, 116, 1998
Mao, S. 1999, *A&A*, 350, L19
Mao, S., et al. 2002, *MNRAS*, 329, 349
Murray, N., Hansen, B., Holman, M., & Tremaine, S. 1998, *Science*, 279, 69
Nemiroff, R.J., & Wickramasinghe, W.A.D.T. 1994, *ApJ*, 424, L21
Perryman, M.A.C. 2000, *Rep. Prog. Phys.*, 63, 1209
Refsdal, S. 1966, *MNRAS*, 134, 315
Rhie, S.H., et al. 1999, *ApJ*, 522, 1037
Sigurdsson, S. 1992, *ApJ*, 399, L95
Smith, M.C. 2003, *MNRAS*, 343, 1172
Soszyński, I., et al. 2001, *ApJ*, 552, 731
Trilling, D.E., Lunine, J.I., & Benz, W. 2002, *A&A*, 394, 241
Udalski, A., et al. 1993, *Acta Astron.*, 43, 289
— 1994, *Acta Astron.*, 44, 227
van Belle, G.T. 1999, *PASP*, 111, 1515
Ward, W.R. 1997, *Icarus*, 126, 261
Witt, H., & Mao, S. 1994, *ApJ*, 430, 505
Yoo, J., et al. 2003, *ApJ*, submitted (astro-ph/0309302)